Plasmonic Oligomers: The Role of Individual Particles in Collective Behavior

Mario Hentschel,[†,‡,*] Daniel Dregely,[†] Ralf Vogelgesang,[‡] Harald Giessen,[†] and Na Liu[§]

[†]4. Physikalisches Institut and Research Center SCoPE, Universität Stuttgart, D-70569 Stuttgart, Germany, [‡]Max-Planck-Institut für Festkörperforschung, Heisenbergstrasse 1, D-70569 Stuttgart, Germany, and [§]Department of Chemistry, University of California, Berkeley, and Materials Science Division, Lawrence Berkeley National Laboratory, Berkeley, California 94720, United States

ABSTRACT We present a comprehensive experimental study of the optical properties of plasmonic oligomers. We show that both the constitution and configuration of plasmonic oligomers have a large influence on their resonant behavior, which draws a compelling analogy to molecular theory in chemistry. To elucidate the constitution influence, we vary the size of individual nanoparticles and identify the role of the target nanoparticle from the spectral change. To illustrate the configuration influence, we vary the positions and numbers of nanoparticles in a plasmonic oligomer. Additionally, we demonstrate experimentally a large spectral redshift at the transition from displaced nanoparticles to touching ones. The oligomeric design strategy opens up a rich pathway for the implementation of optimized optical properties into complex plasmonic nanostructures for specific applications.

KEYWORDS: plasmons · coupling · Fano-resonances · dark mode · oligomer

A particularly important subfield of plasmonics is the study of near-field coupling between noble metal nanostructures. A metal nanoparticle supports localized surface plasmons, which are associated with the collective oscillation of the conduction electrons in the nanoparticle. Such an oscillation can be localized on a single nanoparticle, or it may involve many coupled nanoparticles.[1,2] Just as atoms join together in different combinations and arrangements to form molecules,[3] a diverse range of new materials can be created by combining together artificial atoms into artificial molecules. Interacting nanoparticles in complexes can give rise to interesting collective behavior, which is unattainable in individual nanoparticles.[4−9] Specially, the optical response of these nanoparticle complexes[10−13] greatly depends on the spatial arrangement of nanoparticles (configuration)[14,15] as well as the intrinsic optical properties of individual nanoparticles (constitution).[16]

Plasmonic oligomers with high symmetry such as heptamers are of significant interest due to their fundamental importance as a model system to understand the nature of electromagnetic coupling as well as their remarkable potential in LSPR sensing.[17] Recently, plasmonic heptamers have been experimentally demonstrated using both bottom-up[18] and top-down fabrication techniques.[19,20,36] Top-down approaches such as electron-beam lithography exhibit advantages of accurately controlling the size and shape of nanostructures as well as precisely positioning these nanostructures in space. In particular, the transition behavior from isolated to collective modes in plasmonic heptamers has been successfully investigated by lithographically controlling the distance between interacting nanoparticles. The interference of the superadiant and subradiant modes resulting from the hybridization[21] of the center and satellite nanoparticles gives rise to intriguing Fano effects.[22−24]

Here we take a further step and examine the role of individual nanoparticles for the collective behavior in plasmonic oligomers. A defect nanoparticle is introduced in a heptamer by gradually varying the size of one satellite nanoparticle. Owing to the unique symmetry of plasmonic heptamers, we are able to demonstrate the different contributions of individual satellite nanoparticles by using two perpendicular polarizations. The contribution of the center nanoparticle is also unravelled by successively varying its size. Subsequently, we examine the role of the spatial arrangement of nanoparticles in plasmonic oligomers. Different numbers of satellite nanoparticles are utilized to explore the symmetry requirement for the formation

* Address correspondence to m.hentschel@physik.uni-stuttgart.de.

Received for review November 22, 2010 and accepted February 8, 2011.

Published online February 23, 2011
10.1021/nn103172t

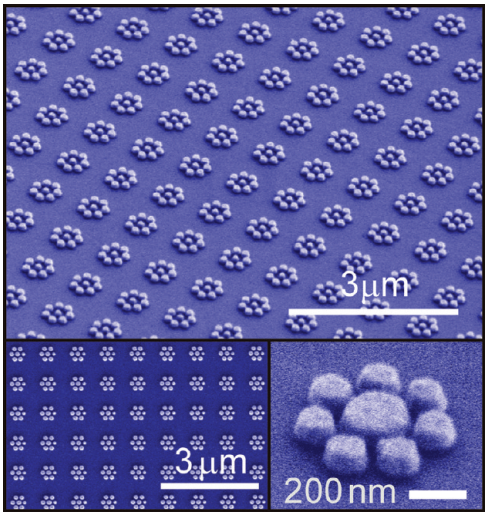

Figure 1. Exemplary SEM images of gold oligomer structures, fabricated by electron-beam lithography. Top: 30° oblique view of an octamer structure. The periodicities in both directions are 900 nm, and the particle height is 80 nm. The diameters of the ring and center particles are 150 nm and 130 nm, respectively. The interparticle distance in the ring is around 30 nm. Bottom left: Normal view of a heptamer structure with a defect. The diameter of the defect particle is around 110 nm. Bottom right: Enlarged view of an octamer structure with a center particle diameter around 230 nm.

of the collective behavior. We show that by carefully engineering the structural symmetry, a plasmonic quadrumer already suffices to generate Fano effects. Our experimental observations represent an important step toward the study of artificial plasmonic molecules with optimized optical properties. Finally, we experimentally demonstrate the intriguing transitional response of a plasmonic heptamer by physically bridging its center nanoparticle with a satellite nanoparticle. Our results constitute the first study of plasmonic encounters using multinanoparticle complexes, which will offer myriad blueprints for studying the resonant behavior of plasmonic systems in the nearly touching regime.[25−28]

RESULTS AND DISCUSSION

We fabricated a series of plasmonic oligomers with different geometries by electron beam lithography on a glass substrate. Figure 1 shows normal and 30° tilted view scanning electron micrographs of selected structures. The footprint of each array is $100 \times 100\,\mu m^2$. The particles forming the outer ring have a diameter of 150 nm, and the center particle has a diameter of 160 nm. The thickness of all the particles is 80 nm. The SEM images demonstrate the good uniformity of the fabricated structures over large areas. The optical response of the plasmonic oligomers for polarization direction as depicted next to the corresponding spectra was evaluated using a Fourier-transform infrared spectrometer. The simulated extinction cross-section spectra and field distributions at the respective spectral positions

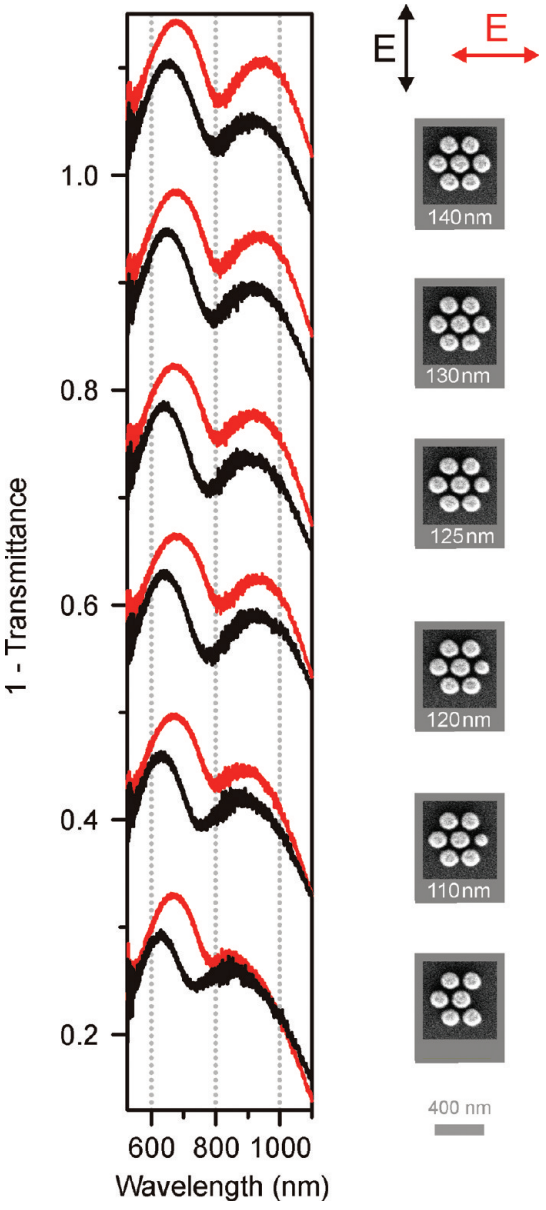

Figure 2. Experimental extinction spectra of the defective heptamer structures in dependence on the defect particle size. The spectra are shifted vertically for clarity. The measured extinction spectra are characterized by red and black curves for the horizontal and vertical polarizations, respectively. Right: Normal-view SEM images of the corresponding structures with indicated defect particle sizes. The scale bar is 400 nm. A successive overall blue-shift of the spectra can be observed for both polarizations. The blue-shift in the vertical polarization is stronger than that in the horizontal polarization.

were calculated using the software package CST Microwave Studio, Darmstadt, Germany (for further details, see the Methods section).

We first study the contribution of an individual nanoparticle in the outer ring to the collective behavior of a plasmonic heptamer. One of the satellite nanoparticles is successively decreased in size until it diminishes completely. The experimental extinction spectra and corresponding SEM images of the

structures are shown in Figure 2. The diameter of the target satellite particle is given below each SEM image. The introduction of the defect nanoparticle gives rise to the drastic reduction of the structural symmetry. The undisturbed heptamer belongs to the symmetry group D_{6h} (C_{6v} if the substrate is considered), whereas the defective heptamer is of $D_{1h} = C_{2v}$ symmetry ($C_{1v} = C_{1h} = C_s$ if considering the substrate). The defective heptamer has only one symmetry axis, which is along the center and the defect particles. The experimental extinction spectra were taken with the electric polarization parallel or perpendicular to this symmetry axis at normal incidence. In the case of the perfect plasmonic heptamer (see the topmost structure in Figure 2), the extinction spectra for the two orthogonal polarizations are nearly identical, as is expected from the symmetry considerations.[11] The slight deviations between the two spectra are likely due to fabrication tolerances in the experiment. The distinct dip in extinction for each polarization, that is, the Fano resonance, is due to the destructive interference between the superradiant and subradiant modes in the plasmonic heptamer. More specifically, the dipolar plasmons in the center particle hybridize with the dipolar plasmons in the outer ring nanoparticles, giving rise to a bright superradiant and a dark subradiant mode. In the superradiant mode, all nanoparticles oscillate in phase, leading to significant spectral broadening due to strong radiative damping. In the subradiant mode, the plasmons in the outer ring nanoparticles and the center particle oscillate antiphase. The unique symmetry of the perfect heptamer allows for similar yet opposite dipole moments in the outer ring and the center particle, hence leading to a spectrally narrow dark subradiant mode. If the super- and subradiant modes spectrally overlap, they can destructively interfere and form a Fano resonance. Its line width is determined by the sharpness of the subradiant mode.

By subsequently introducing the defect, *i.e.*, decreasing the size of one satellite nanoparticle, a significant suppression of the superradiant profile line width is observable for both polarization directions. This behavior can be related to the reduced dipole moment of the superradiant mode due to the successive reduction of the target ring particle size. This effect is polarization independent and can hence be observed in both spectra. Additionally a blue shift of the Fano resonance can be observed. The shift for vertical polarization is stronger than for the horizontal one. To understand the spectral characteristics, the near-field distributions at the respective spectral positions of the structure in which the defect nanoparticle is completely absent are presented in Figure 3. For the excitation polarization along the defect line, the near-field distributions display the horizontal mirror symmetry imposed by the geometry of the structure and closely resemble the field-distributions of the undisturbed heptamer. The removal of the ring particle leads to reduced attractive interaction, explaining the observed blue shift. As the local electric fields associated with the two ring particles along the excitation direction are weak compared to the other five nanoparticles (compare Figure 3A), the influence of its removal is minor. The observed decreased modulation depth of the Fano resonance is due to the reduced dipole moment of the ring mode upon shrinking of the defect satellite nanoparticle. In essence, removing an outer particle along the symmetry axis at this polarization does not strongly influence the formation of the Fano resonance as long as the net dipole moment of the outer ring can be effectively compensated by the dipole moment of the center nanoparticle. For the excitation perpendicular to the

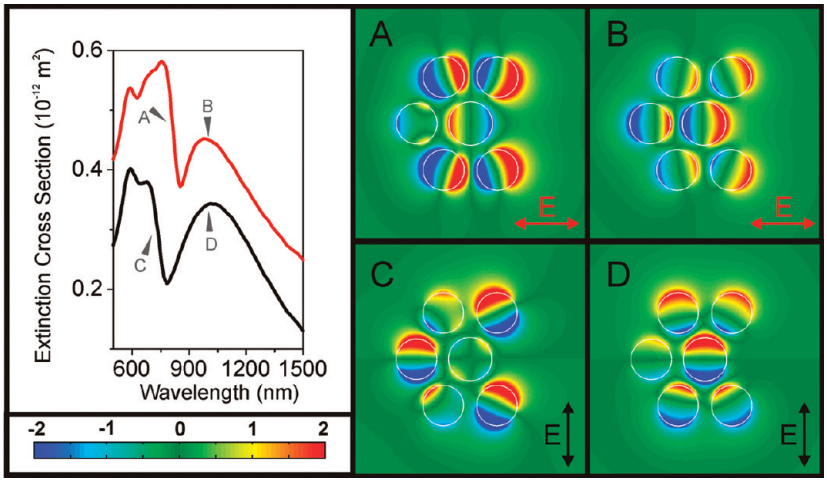

Figure 3. Simulated electric-field distributions (*z*-component, normalized to the incoming field strength) and extinction cross-section spectra of the structure without the rightmost particle. Horizontal polarization: (A) antiphase plasmons are excited in the center particle and the outer particles, in close resemblance to that of the fully symmetric heptamer structure at the Fano resonance; (B) all nanoparticles oscillate in phase. Vertical polarization: (C) quadrupolar field distributions are observed in the center nanoparticle, effectively reducing the attractive interaction and leading to the blue-shift of the Fano resonance with respect to the symmetric case; (D) all nanoparticles oscillate in phase.

defect axis, the field distributions do not show any structural symmetry associated with this axis. Interestingly, at spectral position C quadrupolar field distributions are observed in the center nanoparticle as a result of the broken symmetry in the system. This leads to a reduction of the attractive interaction, which effectively raises the resonance energy and explains the observed strong blue-shift of the Fano resonance.

Our experiment shows that the broken symmetry crucially influences the optical response of the plasmonic heptamer. Depending on the position of the defect relative to the light polarization, the optical response of the oligomers strongly differs, validating the different roles of individual particles on the collective behavior of plasmonic aggregates.

Next, we study the influence of the number of nanoparticles in the outer ring on the optical properties of plasmonic oligomers. Figure 4 shows the experimental extinction spectra and the corresponding SEM images of the plasmonic oligomers with different numbers of particles in the outer rings. The ring and center particle diameters are 150 and 160 nm, respectively. The number of particles in the outer ring is varied from two to six. The constituting particles are equally spaced for each structure. As a result, the interparticle distance decreases in the outer ring when more particles are added.

In the case of the single center particle, a dipolar resonance can be excited. When adding two parallel particles to the center particle, there is still a single

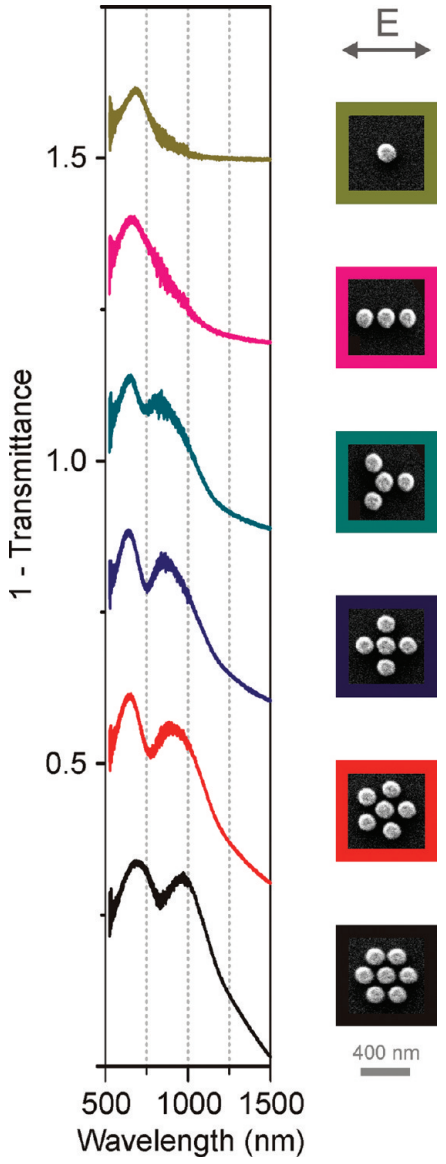

Figure 4. Experimental extinction spectra of the plasmonic oligomers in dependence on the number of particles in the outer ring for horizontal polarization. The spectra are shifted vertically for clarity. Right: Corresponding SEM images. The scale bar is 400 nm. The center and ring particle diameters are 160 and 150 nm, respectively. The particle height is 80 nm. A Fano resonance emerges when the number of ring nanoparticles is increased to three. By further adding ring particles, the Fano resonance's modulation depth increases and the resonance shape becomes more symmetric.

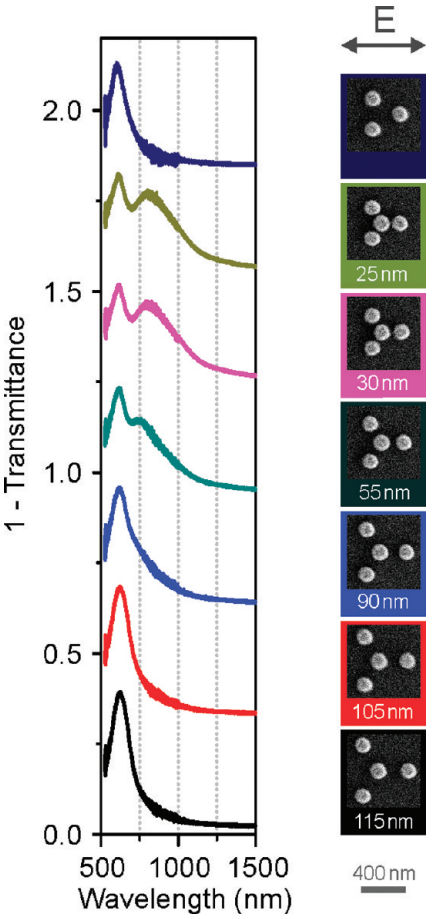

Figure 5. Experimental extinction spectra of quadrumers in dependence on the interparticle separation and a reference trimer. The spectra are vertically shifted for clarity. Right: SEM images of the corresponding structures, the gap between ring and center particle is indicated below. For the largest distances one observes isolated particle-like spectra. Below a gap size of 55 nm (green curve), the signature of a Fano resonance is clearly observable. Its modulation depth increases with decreasing gap size. By removing the center particle the Fano resonance vanishes.

resonance visible which exhibits a broader line width due to a stronger dipole moment. When adding a third particle, the signature of a Fano resonance comes into existence. By further adding particles, the modulation depth of the Fano resonance remarkably increases together with a slight resonance red-shift. In other words, the strength of the Fano resonance can be manipulated by controlling the number of particles in the outer ring. By changing the number of particles in the ring the coupling strength between the particles becomes stronger and the overall number of interacting particles rises. Consequently the dipolar mode of the outer ring is red shifting. As a result the hybridized super- and subradiant modes formed by the red-shifted ring mode and the central particle mode are red-shifted as well. This readily explains the overall shift of the spectra. The red shift of the superradiant mode is stronger then the one of the subradiant mode, hence decreasing the spectral detuning between the two. This manifests itself in an increasing symmetry of the spectrum. The Fano dip is observed right in the center of the broad superradiant mode when there is no detuning. Additionally the dipole moment of the mode in the outer ring is increasing, making it comparable to the one of the center particle. Matching the dipole moments of the outer ring and the center particle is the key to generating a pronounced Fano resonance in the extinction spectrum. Evidently, by carefully designing the structural symmetry, a Fano resonance can be already established in a simple oligomer consisting of only four particles.[30] This behavior can be ascribed to the interaction of two doubly degenerate E-modes—belonging to the $C_{\infty v}$ symmetry of the center particle and the C_{3v} symmetry of the triangular ring—which ensures both group theoretical and geometrical compatibility (see Supporting Information).

To gain further insight about the formation of a Fano resonance in the quadrumer cluster, we fabricated a distance-dependent series. The experimental extinction spectra and corresponding SEM images are shown in Figure 5. The ring and center particle diameters are 150 and 160 nm, respectively. The distance between the center particle and the ring particles is varied between 25 and 115 nm.

For large gap sizes single-particle-like spectra are observed as the particles are not or only very weakly coupled *via* the near-field to one another. For a gap size of 55 nm the signature of a Fano resonance comes into existence. Its modulation depth is increasing for decreasing distance. Strikingly, the Fano resonance vanishes completely when the center particle is removed from the 25 nm gap structure. The resulting trimer spectrum closely resembles an isolated particle spectrum, indicating that the particles are only very weakly coupled. The formation of a Fano resonance is hence only possible because of the coupling of the three ring particles to the center one. The ring particles are too far apart from one another to efficiently interact *via* their respective near fields. This is in contrast to the heptamer structure where the six ring particles can efficiently couple to one another. Upon removal of the center particle the hexamer spectrum still shows evidence of coupling as it does not resemble a single-particle-like spectrum.[19]

Our interpretation is confirmed by extinction cross section and electric field distribution simulations for a 20 nm gap size quadrumer and for a trimer which are shown in Figure 6. For the strongly coupled quadrumer one observes a well-modulated Fano resonance. The

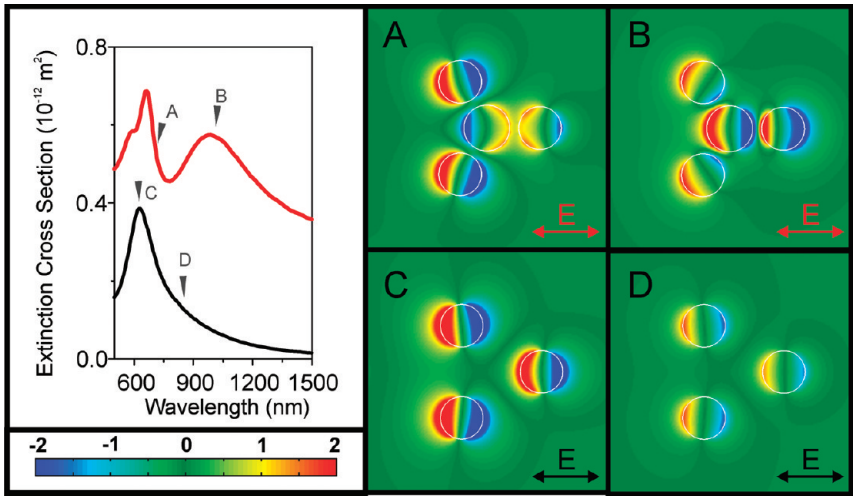

Figure 6. Simulated electric-field distributions (*z*-component, normalized to the incoming field strength, horizontal polarization) and extinction cross-section spectra of a 20 nm gap quadrumer and a trimer that is obtained by removing the quadrumer's center particle. The simulated spectra agree very well with the experimentally obtained spectra of Figure 5. (A) The field distribution shows an out of phase oscillation of the center particle and the three ring particles, which is the signature of the subradiant mode. (B) All plasmons oscillate in phase. Strong coupling between the particles is observed, as is expected for the signature of the superradiant mode. (C and D) Only isolated plasmons are visible in the field distribution. All plasmons oscillate in phase with no observable coupling.

near-field distribution at spectral position A shows a pronounced antiphase oscillation of the plasmons in the ring particles with respect to the center one (subradiant mode). At the long wavelength extinction peak (spectral position B) all particles oscillate in phase as is expected for the superradiant mode. In case of the trimer all particles oscillate in phase and show only very weak mutual coupling (spectral positions C and D). These observations confirm our finding that the collective behavior of the quadrumer cluster is indeed mediated by the center particle alone. Removing it leaves isolated particles showing nearly no near-field coupling.

The center nanoparticle also plays a key role in determining the resonant behavior of plasmonic oligomers. Figure 7 shows the experimental extinction spectra of a series of plasmonic octamers, where seven nanoparticles form the outer ring. The diameter of the center particle is subsequently enlarged from 110 to 230 nm as shown in the corresponding SEM images. For the octamer with a missing center particle, one can observe a broad resonance with a long and unstructured tail toward the longer-wavelength side. A Fano resonance emerges as a kink on the right spectral slope when the center particle diameter is increased to 150 nm. By further enlarging the center particle diameter, the modulation strength of the Fano resonance becomes more pronounced, and the Fano resonance gradually shifts to the red. Also, the resonance profile of the superradiant mode is significantly broadened.

In fact, by increasing the center particle diameter, several structural parameters of the octamer are changed simultaneously. First, due to the decrease of the interparticle distance, the coupling strength between the center particle and the ring particles increases, rendering the formation of the super- and subradiant modes possible. For the cases with center particle diameters smaller than 150 nm, the spectra closely resemble that of the structure without the center particle. Starting from a center particle size of about 150 nm the signature of the Fano resonance comes

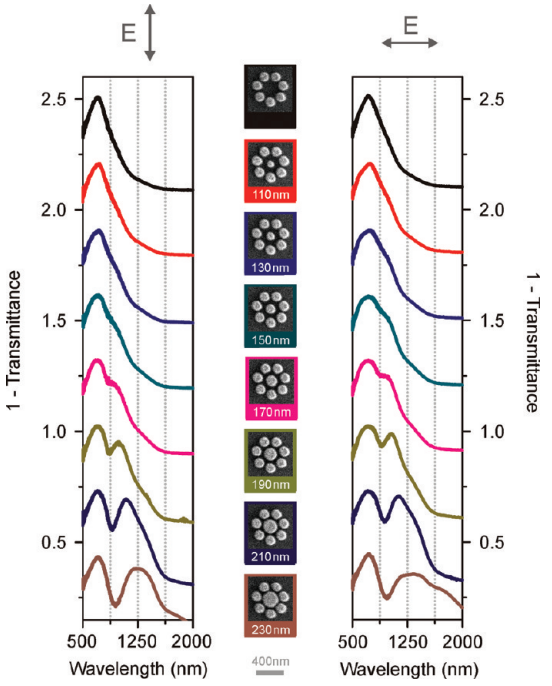

Figure 7. Experimental extinction spectra of the plasmonic octamers in dependence on the center particle diameter for vertical (left column) and horizontal (right column) polarizations. The center particle diameter is indicated in the corresponding SEM images. The scale bar is 400 nm. The signature of the Fano resonance appears when the center particle diameter is increased to 150 nm. The modulation depth is improved with an increase in the center particle diameter. The Fano resonance becomes more symmetric, and the superradiant mode profile is significantly broadened.

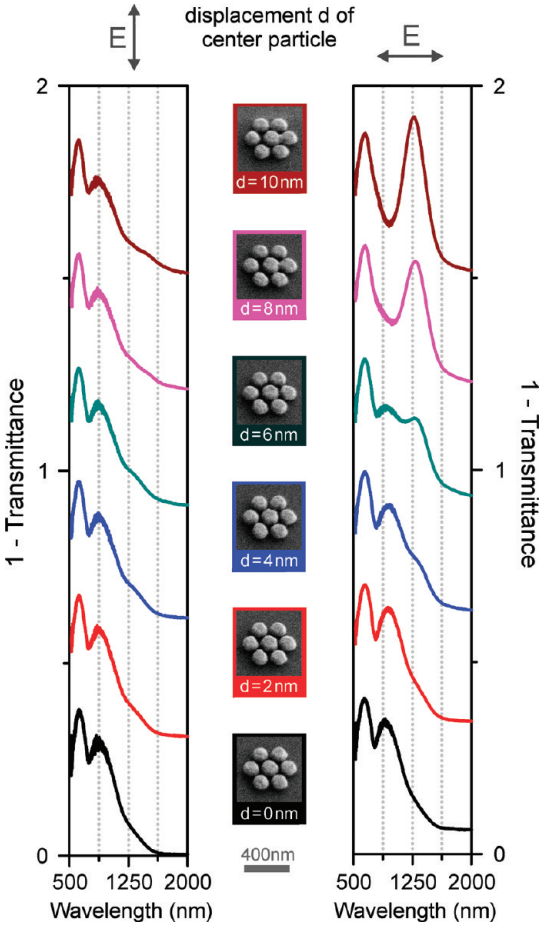

Figure 8. Experimental extinction spectra of the plasmonic heptamer structures in dependence on the lateral displacement of the center nanoparticle to the right for vertical (left column) and horizontal (right column) polarizations. The nominal displacement *d* of the middle particle from its center position is given below the corresponding SEM images (middle column). The scale bar is 400 nm. For the horizontal polarization, a strong new resonance mode appears at a long wavelength and it gains in strength with increasing displacement. This is due to the formation of a conductive bridge between the center particle and the adjacent rightmost particle that are clearly visible in the SEM images. The Fano resonance disappears in the process. For the vertical polarization, the overall spectra are nearly unchanged.

into existence. This behavior shows that the collective super- and subradiant modes have formed. The poor modulation depth of the Fano resonance is hence caused by dipole moment mismatch between center particle and the dipolar ring mode rather than by insufficient near-field coupling. Further increasing the center particle diameter and hence its oscillator strength leads to a better match of the dipole moments. This increases the modulation depth of the Fano resonance. In contrast to the heptamer, the dipole moments are no longer matched in the octamer with equally sized nanoparticles (see the green curve in Figure 7). Second, the resonance position of the center particle shifts to the red due to the increase of the center nanoparticle diameter. This partially accounts for the overall red-shift of the spectrum. Additionally, the red-shift of the center particle resonance reduces the position detuning between the super- and subradiant modes, leading to a more symmetric Fano resonance in the spectrum. The strong spectral broadening is due to the significantly increased overall dipole moment of the superradiant mode upon growth of the center particle. The spectral differences between the two excitation polarizations can be attributed to fabrication tolerances.

Finally, we show that breaking the symmetry of the heptamer by displacing the center particle from its center position enables intriguing resonant behavior. Essentially, using this scheme, one can study the consequence of symmetry breaking as well as the formation of a true defect by physically bridging the center particle and one ring particle. Figure 8 displays the experimental extinction spectra and 30° tilted view SEM images. The nominal displacement *d* is indicated below each SEM image. When the displacement is enlarged (the center nanoparticle is gradually displaced to the right, see Figure 8), more and more center particles within an oligomer array (100 × 100 μm^2 size) touch their adjacent ring particles.

For the incident polarization parallel to the displacement axis, a new pronounced resonance is visible at a long wavelength around 1250 nm. To elucidate the spectral characteristics, field distributions at the respective spectral positions are presented in Figure 9. It is apparent that at resonance B strong dipolar plasmons are excited in the dumbbell-like structure formed by the two touching particles. The neighboring isolated particles mostly oscillate in phase. At this resonance, the spectral response is dominated by the dipolar plasmons in the dumbbell-like particle, which exhibits strong local electric fields as shown in Figure 9B. The amplitude of resonance B increases with enlarging the displacement because more and more dumbbell-like structures are formed in the array. SEM examination of the sample reveals that in the biggest displacement case (see the topmost spectrum in Figure 8), the dumbbell-like structure is formed in nearly every heptamer in the array. The increasing displacement decreases the effective length of the dumbbell-like structure, thus giving rise to the observed blue-shift of resonance B. The Fano resonance is subsequently smeared out by this long wavelength mode and vanishes completely.

Interestingly, the field distributions at the extinction dip (see spectral position A in Figure 9) still exhibit an antiphase plasmon oscillation in the remaining five ring particles and the dumbbell-like defect structure. Nevertheless, due to the strong spectral position

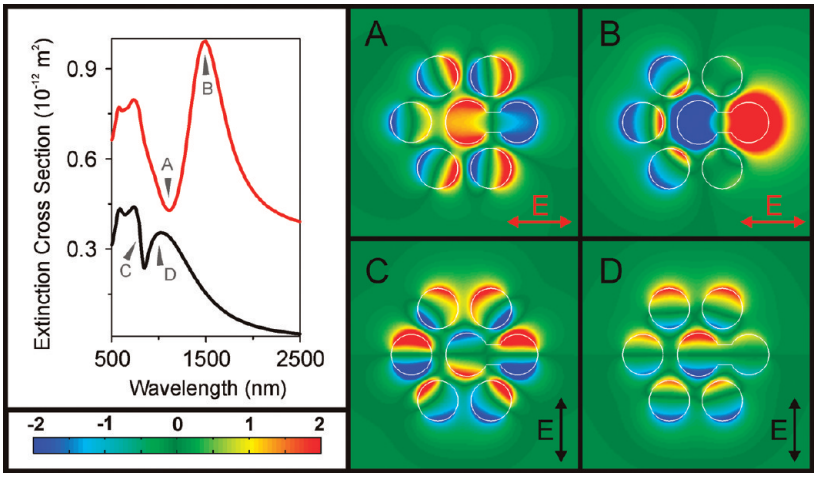

Figure 9. Simulated electric-field distributions (*z*-component, normalized to the incoming field strength) and extinction cross-section spectra of the heptamer structure, in which the center particle is displaced by 10 nm toward the rightmost particle. Horizontal polarization: (A) dipolar plasmons excited in the dumbbell-like structure oscillate antiphase compared to those in the outer ring nanoparticles. Due to the strong mismatch of the resonance positions as well as the dipole moments of the dumbbell-like structures and the outer ring, the Fano resonance cannot be formed (B) fields are mostly confined in the dumbbell-like structure and the plasmons oscillate in-phase with those in the outer ring nanoparticles. Vertical polarizations: (C) similar plasmon oscillations as those in a perfect heptamer at the Fano resonance are observed; (D) all particles oscillate in phase.

detuning and dipole moment mismatch between the defect particle and the ring particles, no Fano resonance is established in this case. In contrast, for the incident polarization perpendicular to the displacement axis, the spectra are mainly unchanged. Even though the center and ring particle touch each other, nearly identical spectral features at the original spectral positions are observed. The corresponding field distributions as shown in Figure 9 panels C and D validate that the plasmon configurations are nearly the same as those of an undisturbed heptamer. Dark-field measurements based on single plasmonic heptamers will be greatly helpful to reveal the effects of the conductive bridge[25−28] by measuring individual structures with different touching junctions.

CONCLUSIONS

We studied the influence of individual particles on the collective behavior of plasmonic oligomers. We found that the defect position within the plasmonic oligomer plays a major role for the optical response. This indicates that particles at different spatial positions contribute unequally. The spectral overlap of the super- and subradiant modes can be tuned by the coupling strength, the center particle size, the outer ring particle size, and the number of ring particles. It is noteworthy that already a three-particle ring around a center particle can closely resemble the spectrum of an undisturbed heptamer. Upon a shift of the center particle toward the outer ring until touching, a pronounced long-wavelength mode appears for the incident polarization along the touching bridge. The Fano resonance diminishes owing to the occurrence of the new mode. On the other hand, for the incident polarization perpendicular to the bridge, the Fano resonance is very robust against the defect introduced by physically connecting the two particles.

For future investigations, we envision plasmonic molecules of increasing complexities. As in molecular physics, atoms join together in different combinations and configurations to form molecules. Analogically, this can be accomplished by using particles with different sizes and even different materials.[31] Metals with different plasma frequencies, for example gold and aluminum disks of an identical size, can lead to different spectral positions of their particle plasmon resonances. This offers an additional degree of freedom to vary the particle resonance position while conserving the structural symmetry of the system. As we have shown, it is possible to design structures of particular symmetries to generate independent spectral features at different polarizations. This might be useful in differential diagnostics applications. Introducing vertical coupling between the oligomer constituents is possible by building three-dimensional artificial plasmonic molecules using a layer-by-layer technique.[32,33] The resulting interaction can be much stronger than lateral coupling. Additionally, the excitation of antisymmetric modes is facilitated by retardation effects.[34,35] It is also remarkable that the electric fields at the Fano resonance are extremely localized in the gaps between the oligomer constituents.[36] This might make our geometry highly useful for practical applications, such as surface-enhanced Raman scattering,[17] plasmonic sensing,[37] higher-order harmonics generation,[38] *etc*.

METHODS

The structures were defined on a glass substrate by electron-beam lithography in a positive resist (PMMA) followed by thermal evaporation of a 3 nm Cr adhesion layer and 80 nm gold followed by a lift-off procedure. The footprint of each array is 100 × 100 μm^2. Electron micrographs of the fabricated structures where obtained by field-emission scanning electron microscopy (SEM), using a Hitachi S-4800. Figure 1 shows 30° tilted and normal incidence images of selected structures under investigation. The particles forming the outer ring have a diameter of 150 nm, and the center particle has a diameter of 160 nm. The thickness of all the particles is 80 nm. The SEM images demonstrate the good uniformity of the fabricated structures over large areas. The slight conical shape of the particles is caused by the lift-off procedure.

The optical response of the plasmonic oligomers was evaluated using a Fourier-transform infrared spectrometer (Bruker IFS 66v/S, tungsten lamp), combined with an infrared microscope (15× Gassegrain objective, numerical aperture NA = 0.4, liquid nitrogen cooled MCT 77 K and Si diode detectors) giving extinction (1-transmittance) spectra. For excitation of the structures, light at normal incidence was used and the polarization direction is depicted next to the corresponding spectra.

The simulated extinction cross-section spectra and field distributions at the respective spectral positions were calculated using the software package CST Microwave Studio, Darmstadt, Germany. An experimentally measured dielectric function of gold was utilized in the simulations.[29] In the calculations, we embedded the plasmonic nanoparticles in a homogeneous medium with an effective refractive index $n = 1.25$ in order to account for the presence of the glass substrate. The assumption of a homogeneous medium is justified as only laterally polarized modes are studied. In the case of out of plane modes the air/glass interface would play a significant role.

Acknowledgment. M. Hentschel, D. Dregely, R. Vogelgesang, and H. Giessen were financially supported by Deutsche Forschungsgemeinschaft (SPP1391 and FOR557), by BMBF (13N9048 and 13N10146), and by Baden-Württemberg Stiftung. N. Liu was supported by the Director, Office of Science, Office of Basic Energy Sciences, of the United States Department of Energy under Contract DE-AC02-05CH11231.

Supporting Information Available: Symmetry tables for different plasmonic oligomers structures. This material is available free of charge *via* the Internet at http://pubs.acs.org.

REFERENCES AND NOTES

1. Barnes, W. L.; Dereux, A.; Ebbesen, T. W. Surface Plasmon Subwavelength Optics. *Nature* **2003,** *424*, 824–830.
2. Maier, S. In *Plasmonics: Fundamentals and Applications*; Springer: Berlin, 2007.
3. Haken, H.; Wolf, H. C. In *Molecular Physics and Elements of Quantum Chemistry*; Springer: Berlin, 2003.

4. Sönnichsen, C.; Reinhard, B. M.; Liphardt, J.; Alivisatos, A. P. A Molecular Ruler Based on Plasmon Coupling of Single Gold and Silver Nanoparticles. *Nat. Biotechnol.* **2005,** *23*, 741–745.
5. Nordlander, P.; Oubre, C.; Prodan, E.; Li, K.; Stockman, M. I. Plasmon Hybridizaton in Nanoparticle Dimers. *Nano Lett.* **2004,** *4*, 899–903.
6. Urzhumov, Y. A.; Shvets, G.; Fan, J.; Capasso, F.; Brandl, D.; Nordlander, P. Plasmonic Nanoclusters: A Path Towards Negative-Index Metafluids. *Opt. Express* **2007,** *15*, 14129–14145.
7. Jun, Y. W.; Sheikholeslami, S.; Hostetter, D. R.; Tajon, C.; Craik, C. S.; Alivisatos, A. P. Continuous Imaging of Plasmon Rulers in Live Cells Reveals Early-Stage Caspase-3 Activation at the Single-Molecule Level. *Proc. Natl. Acad. Sci. U.S. A.* **2009,** *106*, 17735–17740.
8. Alu, A.; Engheta, N. The Quest for Magnetic Plasmons at Optical Frequencies. *Opt. Express* **2009,** *17*, 5723–5730.
9. Brandl, D. W.; Mirin, N. A.; Nordlander, P. Plasmon Modes of Nanosphere Trimers and Quadrumers. *J. Phys. Chem. B* **2006,** *110*, 12302–12310.
10. Quiten, M.; Kreibig, U. Optical Properties of Aggregates of Small Metal Particles. *Surf. Sci.* **1986,** *172*, 557–577.
11. Mirin, N. A.; Bao, K.; Nordlander, P. Fano Resonances in Plasmonic Nanoparticle Aggregates. *J. Phys. Chem. A* **2009,** *113*, 4028–4034.
12. Le, F.; Brandl, D. W.; Urzhumov, Y. A.; Wang, H.; Kundu, J.; Halas, N. J.; Aizpurua, J.; Nordlander, P. Metallic Nanoparticle Arrays: A Common Substrate for Both Surface-Enhanced Raman Scattering and Surface-Enhanced Infrared Absorption. *ACS Nano* **2008,** *2*, 707–718.
13. Gomez, D. E.; Vernon, K. C.; Davis, T. J. Symmetry Effects on the Optical Coupling between Plasmonic Nanoparticles with Applications to Hierarchical Structures. *Phys. Rev. B* **2010,** *81*, 075141.
14. Verellen, N.; Sonnefraud, Y.; Sobhani, H.; Hao, F.; Moshchalkov, V. V.; Van Dorpe, P.; Nordlander, P.; Maier, S. A. Fano Resonances in Individual Coherent Plasmonic Nanocavities. *Nano Lett.* **2009,** *9*, 1663–1667.
15. Bao, K.; Mirin, A. M.; Nordlander, P. Fano Resonances in Planar Silver Nanosphere Clusters. *Appl. Phys. A: Mater. Sci. Process.* **2010,** *100*, 333–339.
16. Halas, N. J. Plasmonics: An Emerging Field Fostered by *Nano Letters*. *Nano Lett.* **2010,** *10*, 3816–3822.
17. Lal, S.; Link, S.; Halas, N. J. Nano-optics from Sensing to Waveguiding. *Nat. Photon* **2007,** *1*, 641–648.
18. Fan, J. A.; Wu, C. H.; Bao, K.; Bao, J. M.; Bardhan, R.; Halas, N. J.; Manoharan, V. N.; Nordlander, P.; Shvets, G.; Capasso, F. Self-Assembled Plasmonic Nanoparticle Clusters. *Science* **2010,** *328*, 1135–1138.
19. Hentschel, M.; Saliba, M.; Vogelgesang, R.; Giessen, H.; Alivisatos, A. P.; Liu, N. Transition from Isolated to Collective Modes in Plasmonic Oligomers. *Nano Lett.* **2010,** *10*, 2721–2726.
20. Lassiter, J. B.; Sobhani, H.; Fan, J. A.; Kundun, J.; Capasso, F.; Nordlander, P.; Halas, N. J. Fano Resonances in Plasmonic Nanoclusters: Geometrical and Chemical Tunability. *Nano Lett.* **2010,** *10*, 3184–3189.
21. Prodan, E.; Radloff, C.; Halas, N. J.; Nordlander, P. A Hybridization Model for the Plasmon Response of Complex Nanostructures. *Science* **2003,** *302*, 419–422.
22. Sonnefraud, Y.; Verellen, N.; Sobhani, H.; Vandenbosch, G. A. E.; Moshchalkov, V. V.; Van Dorpe, P.; Nordlander, P.; Maier, S. A. Experimental Realization of Subradiant, Superradiant, and Fano Resonances in Ringdisk Plasmonic Nanocavities. *ACS Nano* **2010,** *4*, 1664–1670.
23. Liu, N.; Langguth, L.; Weiss, T.; Kästel, J.; Fleischhauer, M.; Pfau, T.; Giessen, H. Plasmonic Analogue of Electromagnetically Induced Transparency at the Drude Damping Limit. *Nat. Mater.* **2009,** *8*, 758–762.
24. Luk'yanchuk, B.; Zheludev, N. I.; Maier, S. A.; Halas, N. J.; Nordlander, P.; Giessen, H.; Chong, C. T. The Fano Resonance in Plasmonic Nanostructures and Metamaterials. *Nat. Mater.* **2010,** *9*, 707–715.
25. Romero, I.; Aizpurua, J.; Bryant, G. W.; Garcia de Anajo, F. J. Plasmons in Nearly Touching Metallic Nanoparticles: Sigular Response in the Limit of Touching Dimers. *Opt. Express* **2006,** *14*, 9988–9999.
26. Lassiter, J. B.; Aizpurua, J.; Hernandez, L. I.; Brandl, D. W.; Romero, I.; Lal, S.; Hafner, J. H.; Nordlander, P.; Halas, N. J. Close Encounters between Two Nanoshells. *Nano Lett.* **2008,** *8*, 1212–1218.
27. Perez-Gonzalez, O.; Zabala, N.; Borisov, A. G.; Halas, N. J.; Nordlander, P; Aizpurua, J. Optical Spectroscopy of Conductive Junctions in Plasmonic Cavities. *Nano Lett.* **2010,** *10*, 3090–3095.
28. Atay, T.; Song, J. H.; Nurmikko, A. V. Strongly Interacting Plasmon Nanoparticle Pairs: From Dipole-Dipole Interaction to Conductively Coupled Regime. *Nano Lett.* **2004,** *4*, 1627–1631.
29. Johnson, P. B.; Christy, R. W. Optical Constants of the Noble Metals. *Phys. Rev. B* **1972,** *6*, 4370–4379.
30. Fan, J. A.; Bao, K.; Wu, C.; Bao, J.; Bardhan, R.; Halas, N. J.; Manoharan, V. N.; Shvets, G.; Nordlander, P.; Capasso, F. Fano-like Interference in Self-Assembled Plasmonic Quadrumer Clusters. *Nano Lett.* **2010,** *10*, 4680–4685.
31. Fredriksson, H.; Alaverdyan, Y.; Dmitriev, A.; Langhammer, C.; Sutherland, D. S.; Zäch, M.; Kasemo, B. Hole-Mask Colloidal Lithography. *Adv. Mater.* **2007,** *19*, 4297–4302.
32. Liu, N.; Guo, H.; Fu, L.; Kaiser, S.; Schweizer, H; Giessen, H. Three-Dimensional Photonic Metamaterials at Optical Frequencies. *Nat. Mater.* **2008,** *7*, 31–37.
33. Liu, N.; Liu, H.; Zhu, S.; Giessen, H. Stereometamaterials. *Nat. Photon* **2009,** *3*, 157–162.
34. Liu, N.; Guo, H.; Fu, L.; Kaiser, S.; Schweizer, H; Giessen, H. Plasmon Hybridization in Stacked Cut-Wire Metamaterials. *Adv. Mater.* **2007,** *19*, 3628–3632.
35. Liu, N.; Fu, L.; Kaiser, S.; Schweizer, H; Giessen, H. Plasmonic Building Blocks for Magnetic Molecules in Three-Dimensional Optical Metamaterials. *Adv. Mater.* **2008,** *20*, 3859–3865.
36. Stockman, M. Dark-Hot Resonances. *Nature* **2010,** *467*, 541–542.
37. Liu, N.; Mesch, M.; Weiss, T.; Hentschel, M.; Giessen, H. Infrared Perfect Absorber and its Application as Plasmonic Sensor. *Nano Lett.* **2010,** *10*, 2342–2348.
38. Kim, S.; Jin, J.; Kim, Y. J.; Park, I. Y.; Kim, Y.; Kim, S. W. High-Harmonic Generation by Resonant Plasmon Field Enhancement. *Nature* **2008,** *453*, 757–760.